Thermochemical Energy Storage for enhancing dispatchability of Solar Photovoltaics

R. Fernández
Escuela Técnica Superior de Ingeniería, Universidad de Sevilla, Camino de los descubrimientos s/n, 41092 Sevilla, Spain
e–mail: rfernandez30@us.es

C. Ortiz
Facultad de Física, Universidad de Sevilla, Avenida Reina Mercedes s/n, 41012 Sevilla, Spain
e–mail: cortiz7@us.es

R. Chacartegui
Escuela Técnica Superior de Ingeniería, Universidad de Sevilla, Camino de los descubrimientos s/n, 41092 Sevilla, Spain
e–mail: ricardoch@us.es

J. M. Valverde
Facultad de Física, Universidad de Sevilla, Avenida Reina Mercedes s/n, 41012 Sevilla, Spain
e–mail: jmillan@us.es

J.A Becerra
Escuela Técnica Superior de Ingeniería, Universidad de Sevilla, Camino de los descubrimientos s/n, 41092 Sevilla, Spain
e–mail: jabv@us.es

ABSTRACT

Solar photovoltaics (PV) plants are today a competitive alternative to power plants based on fossil fuels. Cost reduction in PV modules, scalability (from kW to MW) and ease of installation of PV plants are enabling a rapid expansion of the technology throughout the world. Nevertheless, PV dispatchability still remains as the major challenge to be overcome due to intrinsic variability of solar energy. Most of the current PV facilities lack energy storage while those with storage systems rely on expensive batteries. Batteries are based on elements such as nickel, lithium or cadmium whose scarcity hinder the sustainability of batteries for storing energy in the large scale. This manuscript presents a novel concept to integrate thermochemical energy storage in PV plants. Furthermore, the concept is also directly adaptable to wind power plants in order to store surplus energy. In particular, this paper analyses the suitability of the Calcium-Looping (CaL) process as thermochemical energy storage system applied to large scale PV facilities. The PV-CaL integration works as follows: a part of power produced in the PV plant provides electricity to the grid while the rest is used to supply heat to carry out the calcination of $CaCO_3$. After calcination, the products of the reaction (CaO and CO_2) are stored separately. When power production is required, the stored products are brought together in a carbonation reactor wherein the exothermic reaction releases energy for power production. The overall system is simulated in order to estimate the process behaviour and results show that storage efficiencies of ~40% can be achieved. Moreover, an economic analysis is developed to compare the proposed system with batteries. Due to the low price of natural CaO precursors such as limestone and the longer lifetime of equipment than batteries, the CaL process can be considered as a promising alternative to increase dispatchability in PV plants. Moreover, limestone is abundant and non-toxic, which is an essential requirement for the storage of energy in massive amounts.

KEYWORDS

Global warming, Renewable energies, Photovoltaic (PV), Thermochemical energy storage (TCES), Calcium looping (CaL), dispatchability

INTRODUCTION

Solar photovoltaics (PV) plants are considered as one of the most promising markets in the field of renewable energy [1], with a PV market growth by 50% in 2016 [2]. The size of PV Plants varies depending on the application [3]: from Pico PV systems of few watts used for off-grid basic electrification, to Grid Connected Centralized systems in the range of MWs [4]. The scalability (from kW to MW), ease installation and cost reduction are enabling a fast growing of the PV installed power all around the world, representing the third worldwide largest renewable source after hydro and wind [5]. Technical improvements and economy of scale have resulted in a significant cost reduction of solar photovoltaic (PV) modules, and an intense global growth of PV industry [6]. Nevertheless, dispatchability still remains as a major challenge to be solved due to intrinsic variability of solar energy. The intermittent nature of PV can also cause oscillations in the power system's voltage and frequency, which create new challenges for the integration of PV in the electric power system [7]. Coupling grid connected PV plants to energy storage systems is a possible solution to solve this problem[8], making thus possible to stabilize electricity supply and move production to high prices in peak periods.

Electrochemical Energy Storage Systems (ECES), batteries**,** have been postulated as the best positioned systems for solving dispatchability issues for renewable energy sources (RES) integration. Johan et al. [9] shows the energy efficiency of different batteries technologies, which goes from 85-95% efficiency for Li-ion batteries to 60-65% efficiency for PSB technology. However, and despite the huge expansion of batteries in market [1], the commercial expansion of batteries still faces great challenges for large scale energy storage. Batteries based on materials such as Lithium, Nickel or Cobalt, whose scarcity and environmental impact compromise the technical and economic viability of this technology for massive energy storage around the world. Recently Tesla built a Li-ion battery (100MW/129MWh) as demonstrator of large scale penetration of RES in Australia [35]. However the technology is based on scarce raw materials and in direct competition for them with other applications as the electrical vehicle.

By 2030 the expected PV installed capacity will be nine times higher than in 2013 [10]. In this line, Geth el al. [11] highlight the necessity of large scale storage systems for integrating non-dispatchable RES and exclude battery storage as a realistic candidate to provide bulk energy storage capabilities. In addition to resource scarcity, another major challenge of batteries is to prolong the lifetime of the system. Because of the variability of solar input, batteries are subjected to continuous charge and discharge cycles, which increases their complexity and cost for large scale facilities [10]. On the other hand, pumped hydro storages, which accounts for 99% of the total installed energy stored, is a feasible solution for the massive storage of energy [12]. However, the application of this technology is constrained to special locations with high altitude gradients.

This manuscript presents a novel concept to integrate Thermochemical Energy Storage (TCES) systems in PV plants, as a sustainable and large-scale storage system. Among the TCES systems, the Calcium-Looping (CaL) process, based on the multicyclic calcination/carbonation of $CaCO_3$ has been selected in this work. The CaL process has been recently analysed to enhance dispatchability in Concentrating Solar Power (CSP) plants [13]–[16]. Main advantages of the CaL process for TCES, are i) the high energy storage density of the system [17], the high turning temperature of the carbonation reaction [18], which allows

using high-efficiency power cycles, and iii) the low cost, wide availability and non-toxicity of natural CaO precursors such as limestone or dolomite.

The so-called Electrical Energy Storage – Calcium looping (EES-CaL) system is based on using the power produced for a PV plant to provide heat by Joule effect for carrying out the calcination endothermic reaction, whose products CaO and CO_2 are stored separately by long periods. When energy is required, the stored products are sent to another reactor where by means of the carbonation exothermic reaction is released the stored energy in the chemical bonds. The system is connected to the centralized power system to export electrical power generated in the power block for the discharge of the cycle. The $CaCO_3$ produced in the carbonator is stored to start a new cycle. The main challenge for the CaL process is the progressive decrease of CaO conversion (X) as the number of cycles increases until reaching a residual value. This loss of activity is mainly dependent on temperature, pressure and gas composition in both carbonator and calciner reactors and can be largely mitigated by choosing appropriate conditions [19], [20]. Thermal to electrical efficiencies higher than 40% can be reached in the integration of the CaL process in CSP plants [21], [22]. The EES-CaL system allows exploiting several storage management strategies by just configuring the charging and discharging cycles of the TCES and integrating them with the electrical supplier system (PV plant) and the power system.

This document is structured as follows: firstly, the novel concept for EES based on CaL technology (EES-CaL) is described with particular focus on the PV integration (PV-CaL) charging and discharging decoupled cycles of CaL are analyzed with special attention to storage tanks. Later on, the system is simulated to analyze the daily behavior for each month of the year. Main results are discussed highlighting the importance of managing storage tanks. A brief discussion on economic issues is also introduced to complete this first approach to the EES-CaL concept. Finally, main conclusions are drawn highlighting the most relevant advantages of the system mainly in comparison to batteries.

CONCEPTUAL EES-CAL SYSTEM FOR PV PLANTS

Figure 1 illustrated the conceptual scheme for the EES-CaL system in PV plants (PV-CaL). The system is composed by two well-differentiated and independent charging and discharging cycles with solid storage tanks and CO_2 vessel. The CaL process scheme is based on a recent work [22] where interested readers can find further details on the configuration. The EES process begins by activating the charging cycle, where the endothermic calcination of limestone ($CaCO_3$) takes place. During this operating mode the EES system requires the consumption of electrical power, which is transformed to thermal power by electrical heating coupled to the calciner. Thus, a part of the electrical power generated in the PV system feeds the EES. The calciner, which may be configured as a Fluidized Bed (FB) or as an Entrained-Flow (EF) reactor, operates under atmospheric pressure at 950 ºC to ensure fast decomposition of $CaCO_3$ [14]. In this conceptual approach, full calcination is assumed [16]. Thermal power provided to the calciner is used for increasing the solids temperature up to the reaction conditions and to provide the calcination enthalpy according to Eq 1.

$$CaCO_{3\,(s)} + \Delta H_r \rightarrow CaO_{(s)} + CO_{2\,(g)} \qquad \Delta H_r = 178\ \frac{kJ}{mol} \tag{1}$$

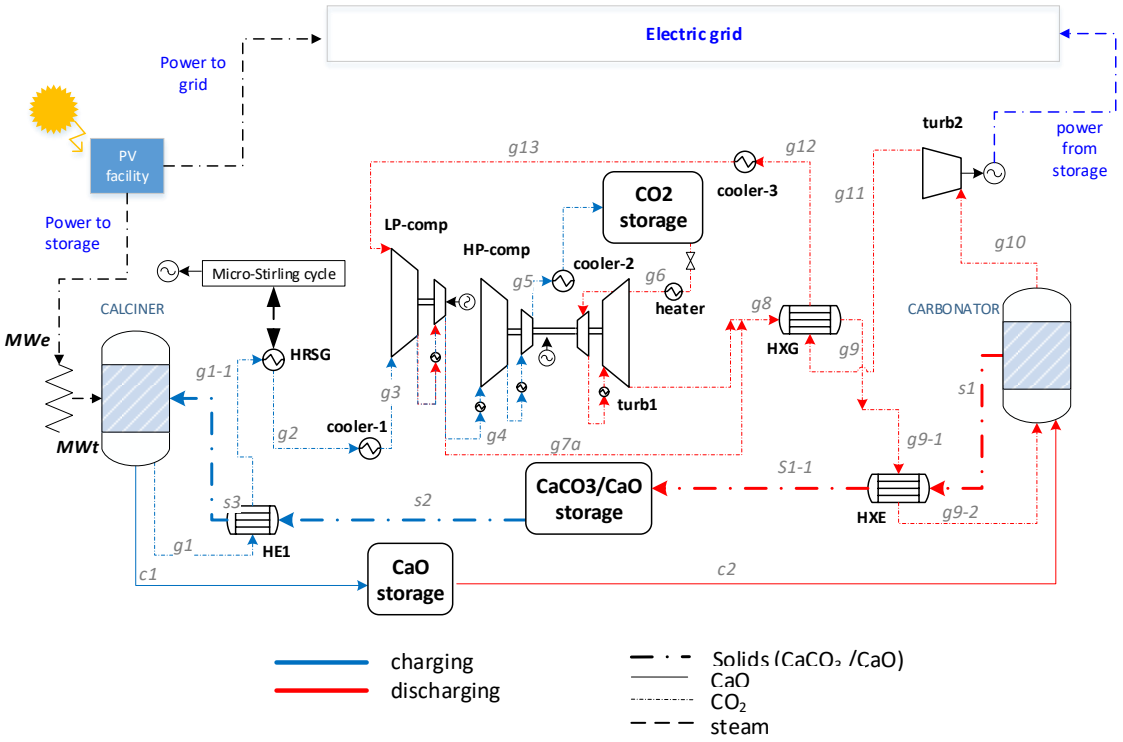

Figure 1. Conceptual scheme for PV-CaL

The $CaCO_3$ entering the calciner is controlled depending on the thermal power provided by the PV system at a given times. The higher the power to the calciner the higher amount of $CaCO_3$ entering the reactor from the solids storage tank. In the tanks solids level is reduced during the charge mode and increased while the discharge mode is active. The CaO produced during calcination is directly stored while the CO_2 is passed through a heat exchanger before being compressed. First, the CO_2 is sent to a cyclonic gas-solid preheater where $CaCO_3$ is heated up. These preheaters are a well-known technology in cement plants [23]. Later, the CO_2 is sent to a Heat Recovery Steam Generator (HRSG) to produce steam within a micro Rankine cycle. The CO_2 stream is further cooled before pressurizing it up to 75 bar [24] by means of an intercooling compressor. The charging cycle ends once the CaO and CO_2 streams produced in the calciner are stored.

The discharging cycle begins when there exists an interest in generating electrical power which has been previously stored during the charge cycle. To activate the discharge cycle, storage tanks start discharging both the CO_2 and CaO streams, which are sent to the carbonator reactor, where the exothermic carbonation occurs. To achieve the desired operation at the exothermic reactor, the control system acts over the mass flow rate of CaO existing the storage tank, which is an independent variable as input for the discharge cycle. The set point of this variable must be set by the control strategy. The CaO mass flow entering in the carbonator determines the total flow rate of CO_2 coming from the storage vessel and thereby the production of $CaCO_3$ in the reactor. The CO_2 at low temperature is passed through a heater before passing it to a turbine to match the carbonator pressure (plus the pressure losses in the CO_2 heat exchangers). After this, the CO_2 stream is passed through a heat exchanger network in order to enter the carbonator at the highest temperature (Figure 1). The amount of CO_2 entering the carbonator is well above the stoichiometric need which allows using the non-reacting CO_2 as heat carrier fluid. As shown in Figure 1, the CO_2 exiting the carbonator at high temperature and pressure and evolves through a thermal turbine to produce

power. In this direct integration the whole system, including charge and discharge processes, constitutes a closed CO_2 Brayton regenerative cycle with elements decoupled in time.
One of the main challenges of CaL process in the progressive CaO deactivation as the number of cycles increases. Previous works have shown however that CaO deactivation is highly dependent on the conditions in the calciner and carbonator reactors (temperature, total pressure, CO_2 partial pressure) as well as on the CaO precursor and their physical properties (particles size, impurities, etc.) [25], [26], and they depend on the application. Thus, a residual CaO conversion as large as X=0.5 may be achieved for carbonation under 100% CO_2 atmosphere and calcination at 725 ºC in absence of CO_2 when using natural limestone with particle size smaller than 45μm [27] Pore plugging limits conversion for larger particles, which in that case reaches a residual value of only X=0.2. [15], [16]. A conservative baseline value of X=0.15 is assumed in the present work for simulating the PV-CaL integration at stationary conditions. Other assumptions about the CaL process scheme have been considered in this work. Turbomachinery efficiency, pressure drops values as well as heat exchangers modelling are presented in [22].

CASE OF STUDY

To illustrate the concept an application of integrated PV-CaL system is developed in this section

PV facility

A detailed simulation of a PV facility located in Seville (Spain) has been performed by using System Advisor Model (SAM) [28]. The PV system is sized for generating 20 MW in DC under 1,000 W/m^2 of total irradiance and cell temperature of 25 ºC. The PV module selected for the PV system is *Sun Power SPR-E19-245* (main characteristics are presented in Table 1) while the selected inverter is *SAM America: CS750CP-US-342V (*Table 2).

Table 1. Module characteristics at reference conditions

Nominal Efficiency	19.169	%
Maximum power (Pmp)	245.025	W_{dc}
Maximum power voltage (Vmp)	40.5	V_{dc}
Maximum power current (Imp)	6.1	A_{dc}
Open circuit voltage (Voc)	48.8	V_{dc}
Short circuit current (Isc)	6.4	A_{dc}
Module area	1.244	m^2

Table 2. Inverter characteristics at reference conditions

Maximum AC power	770000	W_{ac}
Maximum DC power	785145	W_{dc}
Power consumption during operation	1992.12	W_{dc}
Power consumption at night	364.7	W_{ac}
Nominal AC voltage	342	V_{ac}
Maximum DC voltage	1000	V_{dc}
Maximum DC current	1600	A_{dc}
Minimum MPPT DC voltage	545	V_{dc}
Nominal DC voltage	617.789	V_{dc}
Maximum MPPT DC voltage	820	V_{dc}

European weighted efficiency	98.122	%

A number of 26 inverters is required for the system size, 20 MW_{dc}, with a maximum DC power by inverter of 785.14 kW_{dc} (Table 2). Thereby the DC-AC ratio would be 0,999001 at reference conditions. The number of PV modules series-connected (modules per string) is given by the average DC voltage in the inverter (772.5 V_{dc}) and the V_{oc} of modules (Table 1). Thus, a total of 16 modules per string have been calculated for the system. The maximum number of parallel strings for the system is calculated as the maximum DC current in the system (maximum DC current in inverter multiplied by the total number of inverters) divided by the short circuit current in the PV module (I_{sc}). As a result, a maximum of 6500 strings in parallel is obtained. Considering 20MWdc of sizing power of the system and a configuration with 16 modules per string, a total of 5100 strings in parallel are required, resulting in 81600 modules. The final configuration of the system and main parameters at reference conditions are shown in Table 3:

Table 3. PV Power Plant configuration at reference conditions

Modules			Inverters		
Nameplate capacity	19994.04	kW_{dc}	Total capacity	20020	kW_{ac}
Number of modules	81600		Total capacity	20413.77	kW_{dc}
Modules per string	16		Number of inverters	26	
Strings in parallel	5100		Maximum DC voltage	1000	V_{dc}
Total module area	101510.4	m^2	Minimum MPPT voltage	545	V_{dc}
String V_{oc}	780.8	V	Maximum MPPT voltage	820	V_{dc}
String V_{mp}	648	V	Actual DC to AC ratio	0.9987033	

The operation of this PV facility located in Seville has been simulated for one-year. It results in an annual generation efficiency of 18.16%, with annual solar irradiance of 180.44 MWh/year and annual generation of 32.77 MWh/year. Figure 2 shows the results of the simulation along the year (a) and in the peak power day (b).

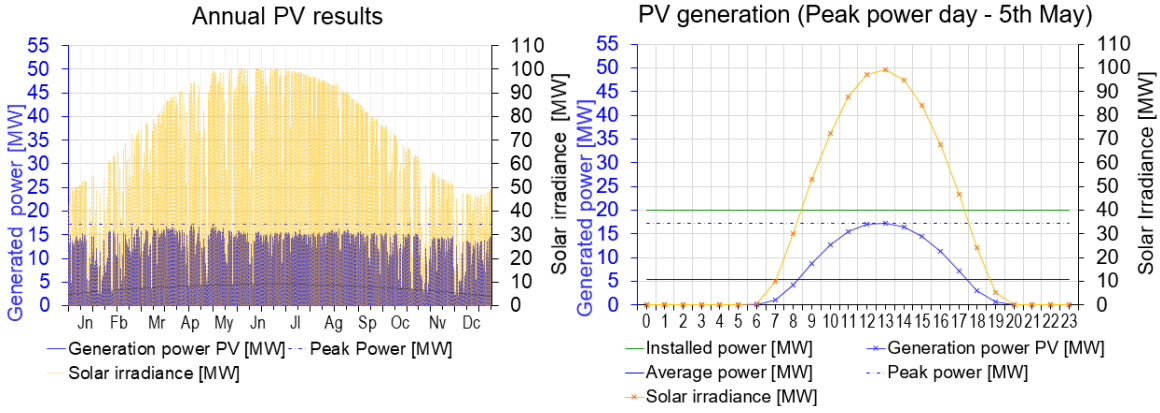

(a) (b)

Note the scales difference between left and right vertical axes.

Figure 2. Simulation results: a) Annual results b) Peak power day results

Figure 1 shows the characteristic intermittent power production linked to seasonal and daily intermittence in solar resource. The PV facility is designed for 20 MW modules capability (under reference conditions), but peak power for the simulated year is 17.3 MW (Figure 2 (a))

since reference conditions and 1000W/m^2 of solar irradiance (nominal conditions) have not been achieved simultaneously to generate 20MW of PV power. The power generation average value is 3.74 MW, which results in 1638 full-load-hours (flh) throughout the year.

PV-CaL process simulation (base case)

The PV-CaL integration shown in Figure 1 has been simulated in order to analyse its potential as electric energy storage system. The integrated PV-CaL system would be in charge of storing the surplus PV generation when the solar resource is not sufficient to generate the target value.

First, a base case is defined. It uses 5 MW_e of electric power produced by the PV system in the CaL process. In the charge period, the use of electric heaters coupled to the calciner allows the calcination of 1.86 kg/s of $CaCO_3$, breaking the chemical bonds to CaO and CO_2. Taking into account that CaO conversion in the carbonation is not complete, in addition to $CaCO_3$, a certain amount of non-reacting CaO from the carbonator enters the calciner and therefore the total amount of solids would be 7.74 kg/s. For the base case analysis, it is assumed that solids exit the storage vessel at 690 ºC. Once calcination occurs, 0.82 kg/s of CO_2 and 6.93 kg/s of CaO are sent to their respective storage tanks. In the energy delivery process, discharge period, the process is modelled assuming that all the stored CaO is sent to the carbonator for releasing the stored power. Table 4 and 5 show main streams data and energy balance of the system results. Nomenclature corresponds to the one used in Figure 1.

Table 4. Main streams data for the PV-CaL integration (base case, 5 MWe from PV to CaL storage)

ID	P [bar]	T [^{0}C]	ṁ [kg/s]	ID	P [bar]	T [^{0}C]	ṁ [kg/s]
s1	3.5	900	7.74	**g5**	75.75	123.65	0.82
s1-1	1.14	689.20	7.74	**g5-2**	75	25	0.82
s2	1.14	689.60	7.74	**g6**	74.25	130	0.82
S3	1.11	719.69	7.74	**g7a**	3.85	78.36	18.01
c1	1	950	6.93	**g8**	3.85	76.80	18.83
c2	1	950	6.93	**g9**	3.66	702.62	18.83
g1	1	950	0.82	**g10**	3.5	900	18.02
g1-1	0.97	719.76	0.82	**g11**	1	718.18	18.02
g2	0.97	70	0.82	**g12**	0.95	91.99	18.02
g3	0.96	40	0.82	**g13**	0.94	40	18.02

The CO_2 stream exits the calciner at high temperature (950 ºC). This high temperature stream is used to increase the temperature of the entering solids up to 720 ºC. This hot CO_2 stream can be used for recovering energy integrating it with a thermal engine aiming to increase the global cycle efficiency and reducing the cooling demand of the system. After this cooling step, the CO_2 stream is compressed up to 75.75 bar before entering the storage tank. Once calcination take places, both the CO_2 and CaO streams previously produced in the calciner are sent to the carbonator reactor. The CO_2 at 75 bar and 25ºC is passed through a heater increasing its temperature up to 130 ºC before passing through the secondary CO_2 turbine. After passing through the heat exchanger network, this stream arrives at 753.24 ºC in the carbonator. With this thermal integration among the streams involved in the process a global efficiency of the plant 39.21% can be obtained (Table 5).

Table 4. Energy balance for the PV-CaL integration (base case, 5 MW_e from PV to storage)

	Parameter	Charging step	Discharging step
Solar thermal power (MW_{th}) from PV to storage		5	0
Heat exchangers thermal Power (MW_{th})	HRSG	0.58	-
	COOLER-1	-0.02	-
	HP-COMP (intercooler)	-0.25	-
	COOLER-2	-0.22	-
	HEATER	-	0.23
	TURB1 (interheater)	-	0.08
	COOLER-3	-	-0.84
	HXG	12.41	12.41
	GS-HE2	1.17	1.17
	GS-HE3	0.50	0.50
	LP-COMP (intercooling)	-	-1.23
Power inlet (MW_e)	CO_2 storage turbine (HPS-TURB)	-	0.11
	Main CO_2 turbine (M-TURB)	-	4.02
	Steam Turbine (ST)	0.12	-
	Main CO_2 compressor (M-COMP)	-0.29	-
	CO_2 storage compressor (HPS-COMP)	-	-1.84
	Auxiliaries heat calciner	-0.004	-
	Auxiliaries solids transport calciner	-0.08	-
	Auxiliaries solids transport carbonator	-	-0.08
W_{net}	$\dot{W}_{net,charge}$ (MWe)	-0.25	-
	$\dot{W}_{net,discharge}$ (MWe)	-	2.21
	Overall plant efficiency (η)	**39.21%**	

Table 5 includes main results from the energy balance in the plant. It shows that with the integration 14.66 MW_{th} have been recovered from the hot streams and integrated into the process, thus increasing the overall efficiency of the plant. Otherwise, there is still a need for extra cooling and heating power of 2.56 MW_{th} and 0.31 MW_{th} respectively.

Global generation in the system is 4.25 MW_e by means of two CO_2 turbines allocated in the discharging cycle and a micro-stirling turbine that recovers thermal power from the hot CO_2 stream exiting the calciner. Energy consumption in the plant (2.28 MW_e) is mainly due to compressors consumption (2.12 MW_e). Note that net energy in the charging process is negative because of the CO_2 compression. As a result of this energy balance, the net generation in the charging and discharging cycle are 2.21 MW_e (net generation) and -0.25 MW_e (net consumption), respectively when the solar thermal power entering in the calciner is 5 MW_e. Considering net electric generation in the system for a given thermal power entering the charging cycle, the overall efficiency of the system is 39.21%.

PV-CaL process design

Once the PV-CaL process configuration has been analyzed for the base case, this section aims to study the daily behavior of the system by considering a quasi-stationary simulation in an hourly basis. Modelling has been carried out without considering off-design conditions. Data

from simulating the PV facility in a typical monthly day (hourly generation considered as the average value of hourly generation for every day of the month) is used as representative of a month base generation. The following storage charging and discharging strategy is used to generate along the day almost constant energy, whose value for each month depends on the available solar resource. The surplus electricity generated in the PV facility over the exported to the grid is used in the charging cycle of the storage system. The CaO and CO_2 used to produce surplus generation hours is distributed along the day to balance the levels in the daily operation. Figures 3 and 4 show the daily PV-CaL performance in a typical July day during charging and discharging, respectively.

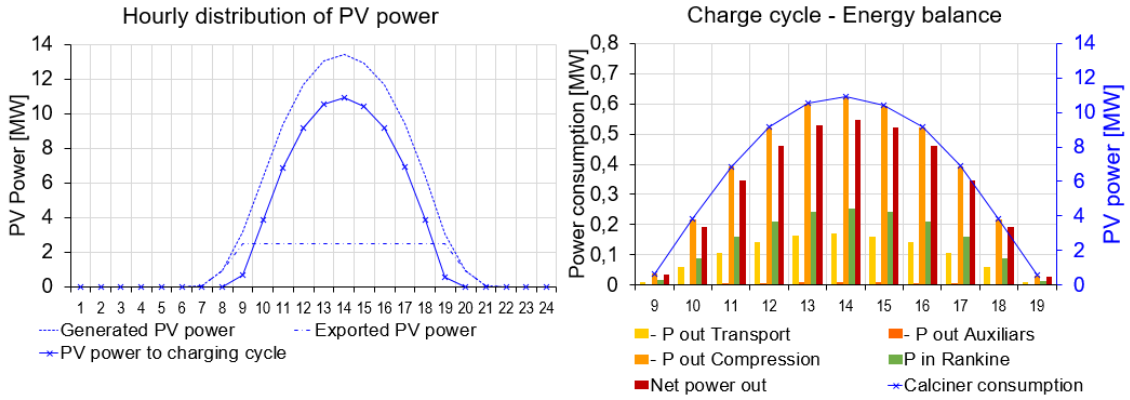

(a) (b)

Figure 3. Charging process: a) Charging strategy; b) Energy balance in the charging cycle

Figure 3 (a) shows the distribution of PV electricity generation during charging hours. Power generation in the PV facility is exported to the grid with a maximum of 2.5 MW_e. When generation exceeds this limit, the surplus electricity is sent to the CaL charging cycle to initiate calcination and storage of reaction products. Operation of this charging cycle implies an energy penalty (Table 5) as shown in Figure 3 (b) where hourly energy balance highlights the net electric power consumption during this operation mode.

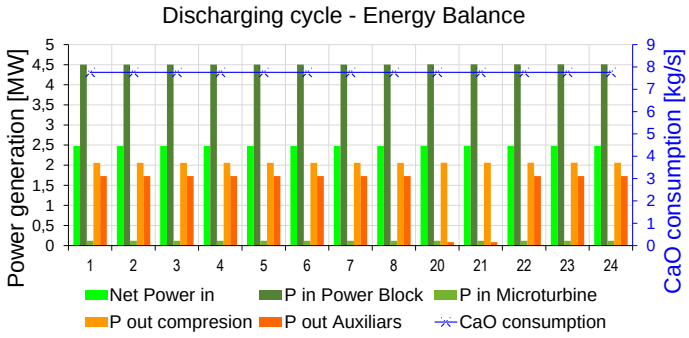

Figure 4. Energy balance in the discharging cycle

When solar resource is not available, the stored CaO and CO_2 as products of calcination are sent to the carbonator within the discharging process, with a strategy of equally distributed. For this application case, with 7.76 kg/s of CaO in the carbonator the net power generation in the cycle is 2.48 MWe. It implies an almost constant power production capacity along the day. As Figure 4 (b) illustrates, despite power generation in the power block is close to 4.5

MW_e, net power generation is strongly reduced due to energy consumption in auxiliary equipment and compression of CO_2 streams.
As result of the energy storage process along a typical July day, energy is stored for 11 hours, from 9:00 to 19:00h. The period of injecting power to the grid is prolonged to 13 hours, allowing to produce a near constant power along the whole day, Figure 5.

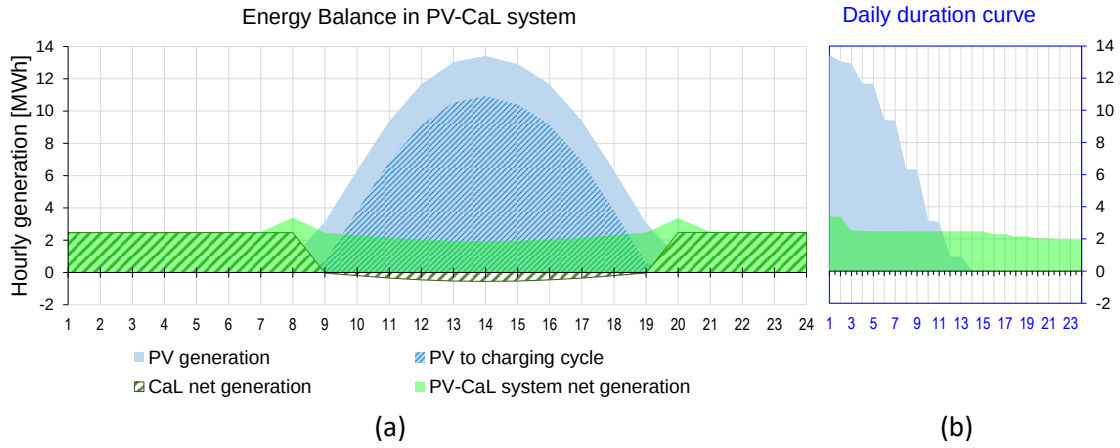

Figure 5. PV-CaL system performance: a) Energy balance in the PV-CaL system. Hourly results; b) Daily duration curve

Figure 5(a) summarizes the energy balance in the PV-CaL system. Net generation during charging hours in the CaL system is negative since the charging cycle is a net energy consumer. Nevertheless, the net generation during discharging hours remains constant at 2.48 MW_e. The PV-CaL system net generation takes into account net generation during discharging hours and PV exported during charging hours. This result is the total energy exported to the grid from the integrated PV-CaL system. The performance of the CaL system obtained is the same than in the base-case, 39.2% (Table 5), since all products from calcination are used in the carbonator. Otherwise, the global performance of the system, which is calculated as the PV-CaL net generation divided by the total PV-generation, is 56.5% and represents a loss of a 44.5% of the total PV-generation due to the storage system. Figure 5 (b) shows a plot the daily duration curve of the PV facility and the PV-Cal system and illustrates the purpose of this strategy, which is conceived to shift intermittent RES generation into almost even and controlled generation.
Storage tanks management is a crucial issue of the PV-CaL system. Figure 6 shows the daily evolution of solids ($CaCO_3$ + CaO), CaO and CO_2 tanks. According to the results, storage capacities of 388.34 tonnes of CaO and 40 tonnes of CO_2 are needed.

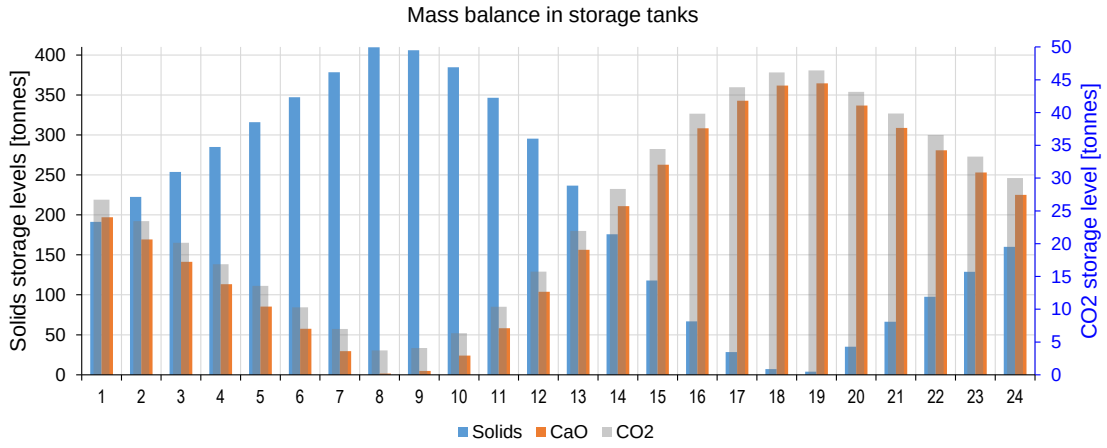

Figure 6. PV-CaL performance. Mass balance in storage tanks

Table 6 shows main results of daily simulation for each month. Monthly base generation represents the design of a system to be integrated with the described PV facility with a strategy of constant production along the whole month.

Table 6. Base PV-CaL generation. Monthly results

Month	**Power generation [MW]**		**Energy balance - Generation [MWh]**				**Global PV-CaL performance**	
	Limit PV	Base discharge	PV to grid)	PV to storage)	CaL to grid	PV-CaL system to grid	C/D [h]	Operation Performance
JAN	1.35	1.33	12.18	45.06	17.69	17.69	9/15	52.17%
FEB	1.5	1.47	14.28	49.98	19.60	19.60	9/15	52.72%
MAR	2.1	2.04	21.56	69.08	27.07	27.07	9/15	53.65%
APR	2	1.91	22.46	60.53	23.72	23.70	10/14	55.65%
MAY	2.3	2.30	26.97	67.71	26.53	26.53	11/13	56.50%
JUN	2.25	2.20	26.87	64.60	25.33	25.33	11/13	57.07%
JUL	2.5	2.48	29.40	72.83	28.55	28.55	11/13	56.69%
AGO	2.45	2.46	27.98	72.41	28.38	28.38	11/13	56.14%
SEP	1.95	1.88	20.66	63.79	25.01	25.01	9/15	54.08%
OCT	1.7	1.69	16.78	57.17	22.41	22.41	9/15	52.99%
NOV	1.2	1.19	10.66	42.87	16.81	16.81	8/16	51.31%
DEC	1.2	1.19	10.31	42.45	16.63	16.63	8/16	51.06%

Design power values goes from 2.48 MW_e in July (most favorable month for PV generation) to 1.19 MW_e in December, being the average achievable base generation 1.85 MW_e. This average value is selected as design power production value to evaluate operation of the system throughout the year.

PV-CaL process daily simulation

Considering the target of 1.85 MW_e generation, when the system is simulated in December (global PV generation of 60.43 MWh/day), the amount of products from the charging cycle is enough to allow generating power at almost constant generation during 19h, achieving a global efficiency in the operation of the system of 54.59%.

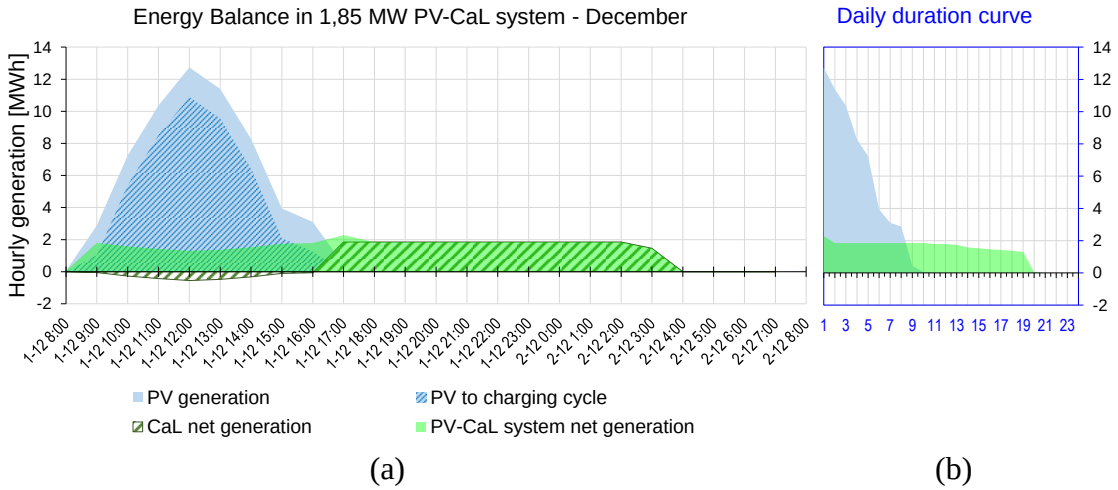

(a) (b)

Figure 7. PV-CaL 1.85MWe system – December: a) Energy balance in the PV-CaL system; b) Annual duration curve

Figure 8 shows the evolution of storage tanks levels along the simulated period. In this case, calcination products are fully consumed along the day and the system is balanced on a daily basis. This is the strategy set for this application but different ones can be considered taken into account the seasonal storage capacity of the CaL system. The minimum required storage capacities are 251.52 tonnes for solids, 26.49 tonnes for CO_2 and 225.03 tonnes for CaO.

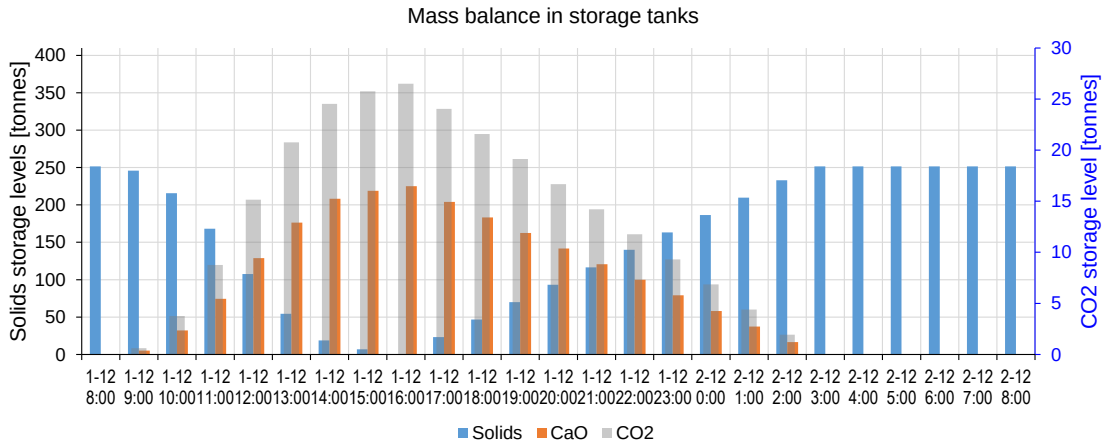

Figure 8. CaL 1.85MWe system – December. Mass balance in storage tanks

The opposite scenario is found in July, which is the most favourable month for PV generation (115.68 MWh/day). Figure 9 shows the performance of the system in this month. During the charging cycle (1.Jul: 9:00 h-19:00h) 454.56 tonnes of CaO are produced and stored before the discharging cycle (1.Jul: 20:00h-2.Jul: 8:00h), which consumes 244.04 tonnes of CaO, thus implying the necessity of extra-storage to address decoupled values of solids and gas streams production and consumption to maintain a strategy of constant power along the whole day.

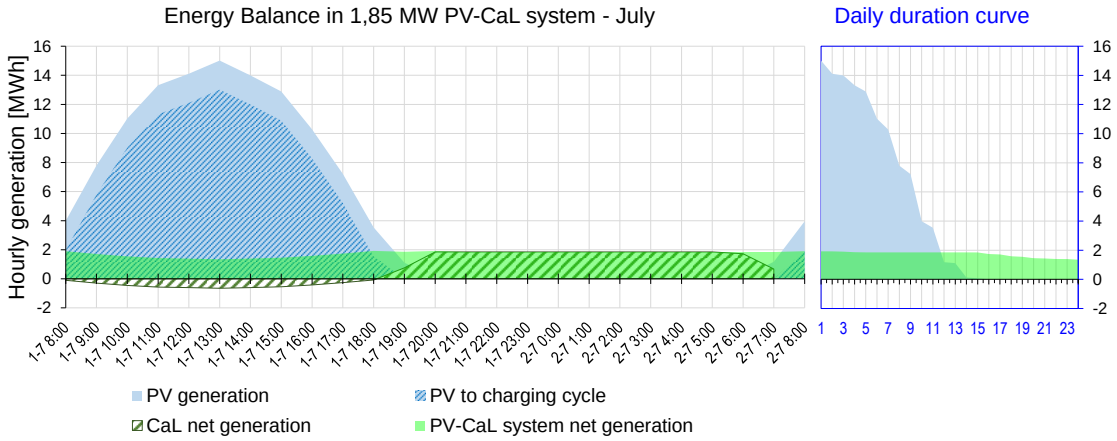

Figure 9. PV-CaL 1.85MWe system – July: a) Energy balance in the PV-CaL system; b) Annual duration curve

Figure 10 shows the mass balance in the PV-CaL system during the operation day. Calcination products are not totally consumed while the consumption of $CaCO_3$ in the calciner is not totally replaced in the discharging cycle thus reducing the level of solids storage tank at the end of the operation day.

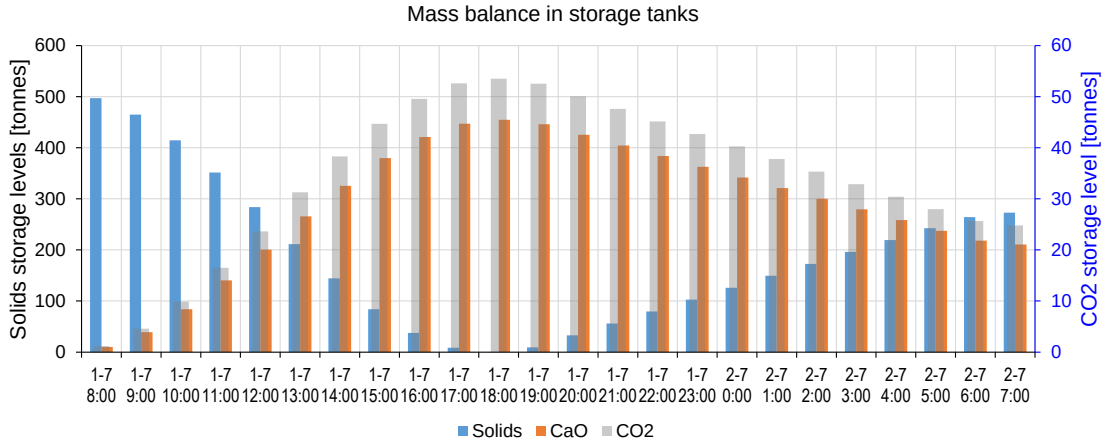

Figure 10. CaL 1.85MWe system – July. Mass balance in storage tanks

ECONOMIC AND SUSTANABILITY ASSESSMENT

A brief economic study has been carried out for the PV system simulated in previous section (Figures 7 and 9). For storage system sizing the month of July has been selected. According to the daily behaviour simulation, 91.18MWhe from the PV facility are charged in the storage system.

In order to estimate the PV-CaL system cost, the methodology proposed in [31] has been followed. Process equipment capital cost has been calculated by using Aspen Capital Cost Estimator [32]. Capital costs of the calciner and carbonator reactors have been estimated according to [33]. Table 7 shows the capital cost estimation for the CaL process as TCES. Because of the novelty of the application and the design effort at this stage, a high contingency cost for the process (15%) and project (30%) has been assumed [31]. The owner cost, which includes feasibility studies, insurance, permitting, land, etc. has been estimated from [32]. Table 8 shows investment costs.

Table 7. Capital cost estimation for CaL

Process equipment [M€]	25.28
Reactors	*12.03*
Storage Vessels	*2.77*
Heat exchangers	*2.45*
Turbomachinery	*5.95*
Solids conveying and separation	*0.47*
Electric heaters	*0.65*
Micro steam cycle	*0.96*
Supporting facilities [M€]	13.65
Piping	*3.09*
Civil	*0.62*
Steel	*0.13*
Instruments	*2.62*
Electrical	*1.98*
Insulation	*0.33*
Paint	*0.17*
Bare Erected Cost (BEC) [M€]	**38.93**
Engineering services [34] [M€]	1.75
EPC cost [M€]	**40.68**
Process contingencies [31] [M€]	6.1
Project contingencies [31] [M€]	12.2
Total plant cost [M€]	**58.98**
Owner cost [M€]	1.18
Total Overnight Cost (TOC) [M€]	**60.16**

Although this estimation yields an elevated investment cost, which is higher than the expected for electrochemical batteries, the proposed concept has a number of relevant advantages for large scale development. It is based on natural CaO precursors (such as limestone), which are among the most abundant materials in Earth. Thus, the raw material employed is widely available, non-toxic, abundant and cheap (~10 $/ton). These essential characteristics for massive energy storage make the PV-CaL concept an attractive technology for the sustainable development of PV power plants without any expected raw material competition with other applications.

CONCLUSIONS

This manuscript presents a novel concept to integrate Thermochemical Energy Storage (TCES) systems using the Calcium-Looping (CaL) cycle in PV plant (PV-CaL system) for electrical energy storage (EES). The work is focused on assessing the operation of the TCES system to address a generation strategy. Different generation strategies could be applied to the system to increase dispatchability of the PV facility. As a first conceptual approach the analysis has been focused on operation of the storage system to keep a constant power generation while the PV generation is variable. The CaL system reaches an efficiency of 39.2% which is low compared to available batteries at large scale whose efficiencies are around 90% [9]. Despite this lower efficiency, the PV-CaL system presents some advantages that make it a very interesting option for sustainable and large-scale energy storage. The PV-CaL system is based on one of the most abundant materials available in nature (limestone,

$CaCO_3$), which circumvents the risk of resource scarcity that may compromise the technical and economic viability of the storage system. This is one of the main advantages that this system presents over current solutions for EES based on chemical batteries. Batteries represent a suitable option for PV and wind storage; however, current materials used in commercial batteries (e.g. Li, Ni, Mn, Co) make them cost intensive whereas the amount of material needed for large-scale applications their storage capability. Another advantage of the integration of the PV-CaL system in the grid for large-scale energy storage is that power is generated mechanically in a CO_2 turbine, a rotatory thermal engine connected to an asynchronous generator that converts mechanical power into electricity (alternating current AC power). This inertial power system results crucial as the size of the system increases due to frequency stability required to the interconnected power grid. The power block and rest of required equipment is easily scalable at the commercial level: two CFD reactors; two solid storage tanks ($CaCO_3$ and CaO); a vessel to store the CO_2 stream in supercritical conditions (75bar and ambient temperature); electrical heating resistors; equipment for solids and gas conveying; instrumentation and control system; and auxiliary systems needed for the correct operation of the system. All these characteristics make the proposed PV-CaL concept an attractive technology for large-scale storage of electric energy.

ACKNOWLEDGEMENTS

This work has been supported by the European Union's Horizon 2020 research and innovation programme under grant agreement No 727348, project SOCRATCES and by the Spanish Government Agency Ministerio de Economía y Competitividad (MINECO-FEDER funds) under contracts CTQ2014-52763-C2, CTQ2017- 83602-C2 (-1-R and -2-R).

REFERENCES

[1] P. G. V. Sampaio and M. O. A. González, "Photovoltaic solar energy: Conceptual framework," *Renew. Sustain. Energy Rev.*, vol. 74, no. March, pp. 590–601, 2017.

[2] International Energy Agency Photovoltaic Power Systems Programme, "Snapshot of global photovoltaic markets 2016," pp. 1–16, 2017.

[3] (IEA) International Energy Agency, *Trends 2016 in Photovoltaic Applications. Survey Report of Selected IEA Countries between 1992 and 2015*. 2016.

[4] REN21, *Renewables 2017: global status report*, vol. 72, no. October 2016. 2017.

[5] A. R. Jordehi, "Parameter estimation of solar photovoltaic (PV) cells: A review," *Renew. Sustain. Energy Rev.*, vol. 61, pp. 354–371, 2016.

[6] A. S. Mundada, K. K. Shah, and J. M. Pearce, "Levelized cost of electricity for solar photovoltaic, battery and cogen hybrid systems," *Renew. Sustain. Energy Rev.*, vol. 57, pp. 692–703, 2016.

[7] M. Karimi, H. Mokhlis, K. Naidu, S. Uddin, and A. H. A. Bakar, "Photovoltaic penetration issues and impacts in distribution network - A review," *Renew. Sustain. Energy Rev.*, vol. 53, pp. 594–605, 2016.

[8] M. Obi and R. Bass, "Trends and challenges of grid-connected photovoltaic systems - A review," *Renew. Sustain. Energy Rev.*, vol. 58, pp. 1082–1094, 2016.

[9] C. J. Rydh and B. A. Sandén, "Energy analysis of batteries in photovoltaic systems. Part I: Performance and energy requirements," *Energy Convers. Manag.*, vol. 46, no. 11–12, pp. 1957–1979, 2005.

[10] IRENA, "Battery Storage for Renewables : Market Status and Technology Outlook," *Irena*, no. January, p. 60, 2015.

[11] F. Geth, T. Brijs, J. Kathan, J. Driesen, and R. Belmans, "An overview of large-scale stationary electricity storage plants in Europe: Current status and new developments,"

Renew. Sustain. Energy Rev., vol. 52, pp. 1212–1227, 2015.
[12] B. Dawoud, E. Amer, and D. Gross, "Experimental investigation of an adsorptive thermal energy storage," *Int. J. energy Res.*, vol. 31, no. August 2007, pp. 135–147, 2007.
[13] G. Flamant, D. Hernandez, C. Bonet, and J.-P. Traverse, "Experimental aspects of the thermochemical conversion of solar energy; Decarbonation of CaCO3," *Sol. Energy*, vol. 24, no. 4, pp. 385–395, 1980.
[14] R. Chacartegui, A. Alovisio, C. Ortiz, J. M. Valverde, V. Verda, and J. A. Becerra, "Thermochemical energy storage of concentrated solar power by integration of the calcium looping process and a CO2 power cycle," *Appl. Energy*, vol. 173, pp. 589–605, Jul. 2016.
[15] M. Benitez-Guerrero, B. Sarrion, A. Perejon, P. E. Sanchez-Jimenez, L. A. Perez-Maqueda, and J. Manuel Valverde, "Large-scale high-temperature solar energy storage using natural minerals," *Sol. Energy Mater. Sol. Cells*, vol. 168, no. March, pp. 14–21, Aug. 2017.
[16] J. Obermeier *et al.*, "Material development and assessment of an energy storage concept based on the CaO-looping process," *Sol. Energy*, vol. 150, pp. 298–309, Jul. 2017.
[17] K. Kyaw, H. Matsuda, and M. Hasatani, "Applicability of Carbonation/Decarbonation Reactions to High-Temperature Thermal Energy Storage and Temperature Upgrading," *J. Chem. Eng. JAPAN*, vol. 29, no. 1, pp. 119–125, 1996.
[18] I. Barin, "Thermochemical data of pure substances VCH, Weinheim (1989)," 1989.
[19] J. M. Valverde and S. Medina, "Limestone calcination under calcium-looping conditions for CO 2 capture and thermochemical energy storage in the presence of H 2 O: an in situ XRD analysis," *Phys. Chem. Chem. Phys.*, vol. 19, no. 11, pp. 7587–7596, 2017.
[20] M. Benitez-Guerrero, J. M. Valverde, P. E. Sanchez-Jimenez, A. Perejon, and L. A. Perez-Maqueda, "Multicycle activity of natural CaCO 3 minerals for thermochemical energy storage in Concentrated Solar Power plants," *Sol. Energy*, vol. 153, pp. 188–199, Sep. 2017.
[21] A. Alovisio, R. Chacartegui, C. Ortiz, J. M. Valverde, and V. Verda, "Optimizing the CSP-Calcium Looping integration for Thermochemical Energy Storage," *Energy Convers. Manag.*, vol. 136, pp. 85–98, Mar. 2017.
[22] C. Ortiz, M. C. Romano, J. M. Valverde, M. Binotti, and R. Chacartegui, "Process integration of Calcium-Looping thermochemical energy storage system in concentrating solar power plants," *Energy*, vol. 155, pp. 535–551, Jul. 2018.
[23] F. Schorcht, I. Kourti, B. M. Scalet, S. Roudier, and L. D. Sancho, "Best Available Techniques (BAT). Reference Document for the Production of Cement, Lime and Magnesium Oxide," 2015.
[24] C. Ortiz, R. Chacartegui, J. M. Valverde, A. Alovisio, and J. A. Becerra, "Power cycles integration in concentrated solar power plants with energy storage based on calcium looping," *Energy Convers. Manag.*, vol. 149, pp. 815–829, Oct. 2017.
[25] A. Perejón, J. Miranda-Pizarro, L. A. Pérez-Maqueda, and J. M. Valverde, "On the relevant role of solids residence time on their CO2 capture performance in the Calcium Looping technology," *Energy*, vol. 113, pp. 160–171, 2016.
[26] B. Sarrion, J. M. Valverde, A. Perejon, L. Perez-Maqueda, and P. E. Sanchez-Jimenez, "On the Multicycle Activity of Natural Limestone/Dolomite for Thermochemical Energy Storage of Concentrated Solar Power," *Energy Technol.*, vol. 4, no. 8, pp. 1013–1019, Aug. 2016.
[27] B. Sarrion, J. M. Valverde, A. Perejon, L. A. Perez-maqueda, and P. E. Sanchez-

jimenez, “On the multicycle activity of natural limestone/dolomite for cheap, efficient and non-toxic Thermochemical Energy Storage of Concentrated Solar Power,” *Energy Technol.*, 2016.
[28] C. National Renewable Energy Laboratory. Golden, “System Advisor Model Version 2017.1.17 (SAM 2017.1.17).” [Online]. Available: https://sam.nrel.gov/content/downloads. [Accessed: 15-Jan-2017].
[29] International Renewable Energy Agency (IRENA), *Electricity storage and renewables: Costs and markets to 2030*, no. October. 2017.
[30] I. Renewable Energy Agency, “Electricity storage and renewables: Costs and markets to 2030,” 2017.
[31] E. S. Rubin *et al.*, “A proposed methodology for CO2 capture and storage cost estimates,” *Int. J. Greenh. Gas Control*, vol. 17, pp. 488–503, 2013.
[32] Aspen Technology Inc, “Aspen Capital Cost Estimator.” 2015.
[33] M. C. Romano *et al.*, “The Calcium Looping Process for Low CO2 Emission Cement and Power,” *Energy Procedia*, vol. 37, pp. 7091–7099, 2013.
[34] Politecnico di Milano – Alstom UK (CAESAR project), “European best practice guidelines for assessment of CO2 capture technologies.,” 2011.
[35] “https://www.tesla.com/es_ES/blog/Tesla-powerpack-enable-large-scale-sustainable-energy-south-australia?redirect=no.” .
[36] T. C. Wanger, “The Lithium future-resources, recycling, and the environment,” *Conserv. Lett.*, vol. 4, no. 3, pp. 202–206, 2011.
[37] “Tesla,” *https://www.tesla.com/es_ES/gigafactory?redirect=no*. .
[38] “https://www.greentechmedia.com/articles/read/is-there-enough-lithium-to-maintain-the-growth-of-the-lithium-ion-battery-m#gs.kln05zU.”
[39] C. Grosjean, P. Herrera Miranda, M. Perrin, and P. Poggi, “Assessment of world lithium resources and consequences of their geographic distribution on the expected development of the electric vehicle industry,” *Renew. Sustain. Energy Rev.*, vol. 16, no. 3, pp. 1735–1744, 2012.